scientific data

Article in Press

Check for updates

OPEN

DATA DESCRIPTOR

Global dataset of plant water transport capacity

Yanchao Zhao *et al.*#

Whole-plant hydraulic conductance (k_{plant}) quantifies the water transport capacity along the soil-plant-atmosphere continuum, and is a key trait determining plant water use and drought response strategies, as well as an essential parameter in ecosystem models. However, globally harmonised data are lacking. Here, we present the "KPLANT Dataset", unifying data from 357 studies including 425 species, spanning 6 continents and multiple biomes, and comprising 3841 observations from 1970 to 2025. The dataset is dominated by woody species (90.71%), particularly trees (81.28%), but also includes graminoids (5.29%), and other growth forms (7 total growth forms). k_{plant} values are given as originally reported, together with water flux and/or water potentials, plant-level dimensional and allometric traits (height, diameter, basal area, leaf area, sapwood area, Huber value) and stand characteristics (plant density, leaf area index, basal area). k_{plant} values are additionally expressed on common normalisation bases, including leaf area, sapwood area, wood area and ground area, as well as on a non-normalised whole-plant basis. We describe the dataset, its strengths and limitations, and provide some examples of its potential uses.

Background & Summary

The plant hydraulic system mediates the uptake, transport, storage, and loss of water along the soil-plant-atmosphere continuum, thereby regulating the plant water balance and contributing substantially to terrestrial ecosystem water and carbon exchange[1,2]. The water transport capacity of this pathway is quantified by the hydraulic conductance of the whole plant (k_{plant}, kg s^{-1} MPa^{-1}), which determines water flux (F, kg s^{-1}) for a given root-to-leaf water potential difference ($\Delta\Psi$, MPa)[3,4]. k_{plant} is an integrative property of plant hydraulic architecture that combines the contributions of roots, stems, branches, and leaves along the flow path[5]. Soil and soil-root interface hydraulic conductances are not directly measured, but they are important components that potentially influence k_{plant} values under unsaturated soil conditions. k_{plant} impacts multiple aspects of plant performance. For instance, during periods of heat and drought, declines in k_{plant} due to xylem damage may lead to plant mortality[6–8], and declines in k_{plant} can constrain carbon assimilation rates by limiting maximum stomatal conductance[9,10]. Thus, k_{plant} is an important parameter in process-based models for predicting stomatal behaviour, plant water use, growth, and drought-induced mortality[11–14].

Despite its importance, k_{plant} remains one of the least systematically quantified components of the plant hydraulic system[15–17]. This is partly because estimating k_{plant} requires concurrent measurements of F and $\Delta\Psi$ at the whole-plant level, quantities that vary over time. This makes k_{plant} more difficult to characterise than organ-level hydraulic traits, which can be more readily measured on excised tissues. Indeed, most hydraulic conductance measurements are obtained at the organ-level, including quantification of the separate contributions of root, stem, branches, and leaf hydraulic conductance, or, more commonly, their path-length and cross-section-normalised conductivities[18–21]. Although organ-level conductivities are closely related to whole-plant water use, they cannot be readily scaled to k_{plant}[22]. Scaling from organ conductivities to whole-plant level is complex due to variability in hydraulic traits along the plant's vertical axis[23,24], substantial uncertainty introduced by allometric scaling, and the involvement of multiple tissues and cell types in water transport through apoplastic and symplastic pathways[4].

In addition, long-term monitoring and comparative assessments of k_{plant} across contrasting environmental conditions and genotypes remain scarce[5,14,18]. This limitation is further compounded by the diversity of methodological approaches used to estimate k_{plant} and by its high variability across ontogeny and plant structure[10,25],

#A full list of authors and their affiliations appears at the end of the paper.

which often hinders data comparison among studies. Previous attempts, including Mencuccini[10] and Wolfe, *et al.*[26], provided valuable foundations but were limited in taxonomic and geographic coverage.

The increasing number of studies reporting either k_{plant} values or the combination of F and $\Delta\Psi$, together with recent works highlighting the central role of k_{plant} in regulating plant water use and responses to soil and atmospheric drought[2,27,28], have motivated this new data compilation initiative. Additionally, some publicly available datasets provide complementary sources for estimating k_{plant}. For instance, the SAPFLUXNET dataset[29] provides global measurements of whole-plant water use based on sap flow that, when combined with measurements of leaf water potential (Ψ_{leaf}) (19 sites currently available), enable the estimation of k_{plant} across species from diverse climates and biomes.

Here, we present a dataset compiling k_{plant} measurements under conditions approaching maximum hydraulic capacity, either estimated directly or calculated from source variables, from 357 studies, encompassing 3841 observations across 425 species and 245 genera. The dataset spans multiple biomes across six continents, covering woody and herbaceous species across seven growth forms (tree, shrub, liana, graminoid, forb, stem succulent, and fern). Data were compiled from peer-reviewed publications, theses, and publicly available studies following a standardised extraction protocol. The dataset includes k_{plant} values, the methods used to estimate them, the underlying F and $\Delta\Psi$ measurements, and plant and stand-level allometric traits (height, diameter, basal area, leaf area, sapwood area, Huber value, plant density and leaf area index) when reported. Many studies included repeated observations reflecting temporal or treatment variation. These are retained and identifiable through the associated metadata. However, systematic coverage of drought-induced conductance loss is not provided; users interested in hydraulic vulnerability should consider that k_{plant} under water stress may be substantially lower. The dataset enables comparative analyses of k_{plant} across and within taxa and with hydroclimatic variability and experimental conditions. It also allows evaluations of k_{plant} at large scales[11,16,30], and fulfils a long-standing demand from plant hydraulics modellers[31]. When measurements are unavailable, k_{plant} has traditionally been estimated by upscaling organ-level values and making many assumptions regarding unmeasured organs. This dataset will help constrain those estimates to improve process-based model predictions of vegetation functioning. Information on the availability of complementary functional traits in source publications is also provided. All data underwent quality control including validation of the data types reported, geographic coordinate checks and verification of unit conversion.

Methods

Dataset construction comprised five stages (Fig. 1): bibliographic search and screening, data extraction and derivation of k_{plant}, scaling and unit standardisation, and quality control.

Bibliographic search and screening. A comprehensive literature search was conducted in February 2025 in Web of Science following the publication indexing terms specified for the search (Table 1). Our search yielded 1,980 publications; the search record is available at: https://www.webofscience.com/wos/alldb/summary/001fec63-0ba1-44c9-a88d-1f28a37a55ee-0147749ab5/relevance/1. Following literature search, the data compilation effort involved 56 participants. A detailed protocol specifying the compilation procedures is provided in the Zenodo repository.

During the initial screening, both the main text and the supplementary materials of the publications were assessed. We excluded studies that did not report either k_{plant} values, or simultaneous measurements of F and paired measurements of predawn leaf water potential ($\Psi_{predawn}$) or soil water potential (Ψ_{soil}) and midday leaf water potential (Ψ_{midday}), as well as those presenting only model-simulated k_{plant}. Literature reviews were included only if they provided new data. With these criteria, 330 publications out of the 1,980 were selected for data extraction. In addition, 27 publicly available k_{plant} studies were contributed by co-authors, including 19 studies derived from SAPFLUXNET.

Data extraction and derivation of k_{plant}. Publications were allocated among data extraction participants, and when participants were co-authors of a source publication, that publication was assigned to them. The extracted data were reported in a standardised Excel spreadsheet template, and the Extraction_template is available in the Zenodo repository. Each participant received a copy of the template. Completed templates were treated as independent studies, each with a unique ID, and were submitted to the coordination team for quality control before integration into the final dataset.

Data were extracted from text, tables, or figures in the main manuscript and/or the supplementary materials. When data were presented in figures, we used WebPlotDigitizer (https://automeris.io/WebPlotDigitizer/) to extract the data. k_{plant} was reported in different formats across publications: as a function of time (e.g. diurnal or seasonal measurements), or for specific treatments, individuals or sites, either as disaggregated observations or as aggregated values (e.g. means).

We extracted k_{plant} values prioritising periods of high transpiration demand (typically midday during peak growing season under non-limiting soil water). When data were reported for multiple treatments, individuals, sites, or time points, all observations were kept at the resolution provided in the source publication. All relevant metadata (e.g. treatment, measurement date, soil water status) are provided to enable appropriate filtering.

When k_{plant} was not explicitly reported, we calculated it from the maximum instantaneous midday F and the concurrent $\Delta\Psi$ for each treatment or aggregation level.

In such cases, k_{plant} was calculated using either the ratio or slope method. For paired F and $\Delta\Psi$ measurements, the ratio method was applied:

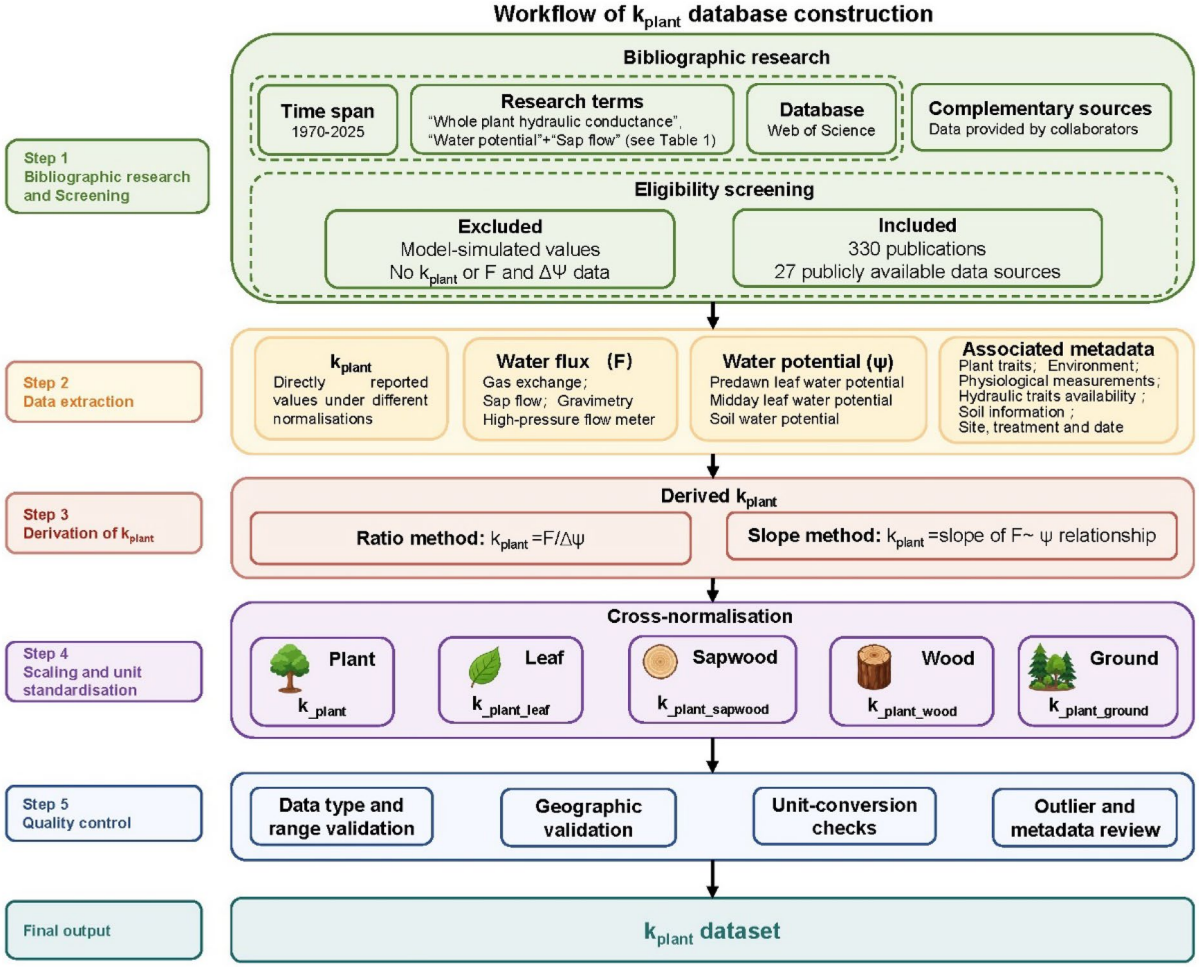


Fig. 1 Workflow of k_{plant} dataset construction.

$$k = \frac{F}{\Delta\psi} \tag{1}$$

When data allowed to plot linear relationships between instantaneous F and instantaneous Ψ_{leaf}, the slope method was applied:

$$F = a + b\psi_{leaf} + \epsilon \tag{2}$$

taking the slope b as the estimate of k_{plant}, a as the intercept (e.g. accounting for capacitance effects) and ϵ representing the residual error.

F data included sap flow (*SF*), transpiration (*E*) measured using gas exchange systems, porometers, or gravimetric water balance methods, and flow rates measured using the high-pressure flow meter (*HPFM*). $\Delta\Psi$ was calculated as the difference between $\Psi_{predawn}$ or Ψ_{soil} and Ψ_{midday}. When multiple F methods were reported, we prioritised *SF*, followed by *E*, and finally the water balance methods and *HPFM*, as *SF* provides more direct and continuous measurements of whole-plant F under field conditions. When both $\Psi_{predawn}$ and Ψ_{soil} were reported, we prioritised $\Psi_{predawn}$ over Ψ_{soil} because it reflects the bulk soil Ψ experienced by the entire root system, whereas Ψ_{soil} is typically measured at specific depths or locations that may not represent the rooting zone. Since we targeted measurements during periods of maximum transpiration rates, deviations from soil-plant equilibrium at predawn (i.e. between $\Psi_{predawn}$ over Ψ_{soil}) are expected to be minimal.

All variables and their associated standard errors (when available) were recorded in their original units and then standardised (Tables 2 and 3, see below). F and water potential data ($\Psi_{predawn}$, Ψ_{soil} and Ψ_{midday}) were included regardless of whether k_{plant} was directly extracted or calculated. Directly extracted k_{plant} values were prioritized over calculated values when both were available.

In addition to k_{plant} (Table 3), $\Psi_{predawn}$, Ψ_{soil}, Ψ_{midday}, and F measurements (Table 2), we recorded the following metadata on site and experimental conditions, including location and sampling date (Table 4); plant-scale and stand-scale characteristics, including taxon and growth form (Table 5); and soil information, concurrent environmental and physiological measurements, and data availability of other hydraulic traits in the original

Water potential (ψ)	Water flux (F)	Hydraulic conductance or resistance
—	—	Whole plant hydraulic conductance
—	—	Hydraulic plant conductance
—	—	Whole plant hydraulic conductivity
—	—	Hydraulic conductance
—	—	Leaf specific hydraulic conductance
—	—	Total hydraulic conductance
—	—	Whole tree hydraulic conductance
—	—	Whole tree hydraulic conductivity
—	—	Soil to leaf conductance
—	—	Soil to leaf hydraulic conductance
—	—	Tree conductivity
—	—	Plant conductivity
—	—	Soil to canopy conductance
—	—	Whole plant hydraulic resistance
—	—	Whole tree hydraulic resistance
—	—	Soil to leaf resistance
—	—	Soil to canopy resistance
Water potential	Sap flow	—
Water potential	Sap flux	—
Water potential	Sapwood water balance	—
Water potential		Resistance to flow
Xylem water potential	Transpiration	—

Table 1. Literature search words.

publications (Table 6). We also recorded data extraction details, including the data extractor name, DOI, publication title, and notes (Table 7).

The descriptions of variables with their default values are shown in the Extraction_template. All numeric variables were standardised to specified units (Tables 2–6). When allometric values were only reported as ranges, we used their mean values for our metadata. When measurement dates were reported as ranges, both starting and ending dates were recorded.

Scaling and unit standardisation. The k_{plant} values reported in publications were in different units and followed different normalisation levels. They could be leaf-area specific, sapwood-area specific, wood-area specific, and ground-area specific hydraulic conductance, or simply per plant (without area normalisation). We recorded the original normalisation level for k_{plant} as "normalisation_level" and retained original k_{plant} values as reported. Then, we standardised the original units to kg m^{-2} s^{-1} MPa^{-1} for the leaf (k_{plant_leaf}), sapwood ($k_{plant_sapwood}$), wood (k_{plant_wood}) and ground (k_{plant_ground}) specific hydraulic conductance, and to kg s^{-1} MPa^{-1} for the overall whole-plant hydraulic conductance without area normalisation (k_{plant}). Where allometric or stand metadata were available we performed conversions to other levels. For example, $k_{plant_sapwood}$ and k_{plant_leaf} were multiplied by plant sapwood area (*pl_SA*) or plant leaf area (*pl_LA*), respectively, to obtain k_{plant}. Similarly, k_{plant} was divided by plant basal area (*pl_basal_area*) or multiplied by stand density (*st_density*), to obtain k_{plant_wood} and k_{plant_ground}, respectively. The normalisation_level variable identifies the normalisation basis reported in the original study and can therefore be used to distinguish directly standardised values from values derived through cross-normalisation, which carry additional uncertainty due to assumptions and additional measurement errors embedded in allometric conversions. All possible conversion combinations are summarised (Table 8).

If possible, we interconverted plant allometric characteristics:

(1) Interconversion between *pl_basal_area* and diameter at breast height (*pl_DBH*) assuming a circular cross-section area:

$$\text{pl_basal_area} = \pi\left(\frac{\text{pl_DBH}}{2}\right)^2 \tag{3}$$

(2) Interconversion among *pl_SA*, *pl_LA*, and *pl_huber_value*:

$$\text{pl_huber_value} = \frac{\text{pl_SA}}{\text{pl_LA}} \tag{4}$$

(3) Conversion between plant and stand level parameters using *st_density*, including transformations between *pl_basal_area* and *st_basal_area*, as well as between *pl_LA* and *st_LAI*.

Field name	Definition	Data type	Units	Possible range	Number of observations
wp_leaf_midday	Leaf water potential at midday	numeric	MPa	<0	2296
wp_leaf_predawn	Leaf water potential at predawn	numeric	MPa	<=0	2250
wp_soil	Soil water potential	numeric	MPa	<=0	466
wp_soil_depth	The depth of soil water potential measurement	numeric	m	—	112
wp_leaf_midday_standard_error	The standard error of leaf water potential at midday	numeric	MPa	—	914
wp_leaf_predawn_standard_error	The standard error of leaf water potential at predawn	numeric	MPa	—	782
wp_soil_standard_error	The standard error of soil water potential	numeric	MPa	—	75
deltaWP	Water potential difference (predawn/soil-midday)	numeric	MPa	>0	2142
WaterFlux	Water flux required to calculate *k*	numeric	Original units	>0	1962
WaterFlux_standard_error	The standard error of water flux	numeric	Original units	>=0	745
Flux_original_units	Units of water flux as given in reference	string	Original units	—	2020

Table 2. Water potential and water flux variables.

$$\text{pl_basal_area} = \text{st_basal_area}/(\text{st_density}) \quad (5)$$

$$st_{LAI} = pl_{LA} \times st_{density} \quad (6)$$

Quality control. Following the data extraction phase, we applied a quality control (QC) to each individual dataset. We implemented an automatic procedure in R (available at https://github.com/vflo/Kwp_QC), to generate reports performing three checks:

(1) Data type and range validation: variables were verified as either numeric or text, and numerical values falling outside pre-established plausible ranges (Tables 2–6) were flagged as potential outliers or input errors.
(2) Geographic validation: country names and geographic coordinates were cross-checked for consistency.
(3) Unit conversion check: based on the original k_{plant} normalisation level and units, and the allometric and stand characteristics available, all possible unit conversion pathways were listed and verified.

Identified errors were corrected and the QC performed again until no issues remained.

After completing QC for each individual dataset, all the data were consolidated into a single dataset. We performed an outlier detection on this dataset, flagging values below the 5th percentile or above the 95th percentile for each numerical variable. Flagged values were reviewed; when errors were confirmed, values were corrected in the individual studies. Missing values in compulsory variables (Tables 3 and 5) were addressed by revisiting original publications. Species names were standardised using the "taxize" R package[32] with the Global Biodiversity Information Facility (GBIF) backbone taxonomy[33]. Original names as reported in source publications were retained in *pl_species_original*, while standardised accepted names were recorded in *pl_species_corrected*. Synonyms were updated to currently accepted names. We also added the species family (*pl_family*) and the GBIF id (*GBIF_id*).

Data records

The dataset is available through Zenodo[34]. The repository contains the main dataset and associated supporting files (Table 9).

Data overview

The KPLANT dataset contains 3841 observations from 357 datasets across 425 species and 245 genera, representing 100 plant families. Observations span 6 continents (Fig. 2a). Europe is the most represented region with 123 studies across 14 countries (1375 observations; 35.80%), followed by North America with 100 studies across 5 countries (767 observations; 19.97%). The dataset includes 2788 observations from field studies, 574 from greenhouse experiments, 129 from plantations, and 350 from outdoor potted plant experiments. The studies span all terrestrial biomes (Fig. 2b). Data from woodland/shrubland were the most numerous, while tropical rainforests, temperate rainforests, and boreal forests are underrepresented.

The dataset covers seven plant growth forms: trees, shrubs, lianas, graminoids, forbs, and stem succulents. Woody species (trees, shrubs and lianas) account for 81.28% of observations with trees representing 80.39% of the dataset. The most represented genera are *Pinus* and *Quercus*, with 507 observations (13.20%) and 489 observations (12.73%), respectively. The most frequently sampled species are *Quercus ilex*, *Robinia pseudoacacia* and *Olea europaea*, with 217 (5.65%), 211 (5.49%) and 167 (4.35%) observations respectively.

The k_{plant} values included in the dataset were originally reported at different normalisation levels: leaf-area specific (52.72%), sapwood-area specific (24.94%), whole-plant (21.11%), wood-area specific (0.60%), and ground-area specific (0.62%). k_{plant} was derived using either the ratio method (89.56%) or the slope method (10.44%). *F* measurements included sap flow (61.70%), infrared gas analyser (20.62%), porometry (10.86%), gravimetry (6.38%), and HPFM (0.44%). Within sap flow methods, thermal dissipation was most common

Field name	Definition	Data type	Units	Possible range	Number of observations
normalisation_level*	Organ area by which the original whole-plant hydraulic conductance is normalised	factor	—	—	3841
Aggregation*	Aggregation level of the data, either temporal, stand or individual. If measures from several days were reported as an average whether for a single tree or across multiple trees, it is named "temporal"; if they were averaged from different trees in one day, it is named "stand"; and if they were averaged from different leaves/shoots it is named "individual".	factor	—	—	3793
N	Number of plant individuals sampled (sample size)	numeric	Number of individuals	>0	3378
k_original*	Leaf, sapwood or whole-plant hydraulic conductance	numeric	Original units	>0	3841
k_standard_error	The standard error of leaf, sapwood or whole-plant hydraulic conductance	numeric	Original units	>0	1222
k_original_units*	Units of whole-plant hydraulic conductance as given in reference	string	Original units	—	3841
k_plant_leaf	Leaf-specific hydraulic conductance in standard units	numeric	kg mLeaf-2 MPa^{-1} s^{-1}	>0	2869
k_plant_sapwood	Sapwood-specific hydraulic conductance in standard units	numeric	kg $msapwood^{-2}$ MPa^{-1} s^{-1}	>0	1681
k_plant_wood	Wood-specific hydraulic conductance in standard units	numeric	kg $mwood^{-2}$ MPa^{-1} s^{-1}	>0	2155
k_plant_ground	Ground area-specific hydraulic conductance in standard units	numeric	kg $mground^{-2}$ MPa^{-1} s^{-1}	>0	1562
k_plant	Whole-plant hydraulic conductance in standard units	numeric	kg MPa^{-1} s^{-1}	>0	1243
k_method*	Method used to estimate whole-plant hydraulic conductance from sap flow	factor	—	—	3841
Flux_method*	Method used to estimate the water flux	factor	—	—	3841
SF_method	Sap flow method	factor	—	—	2374

Table 3. k_{plant} related variables. Compulsory variables are marked with an asterisk (*). Variable names with the underscore after *k* indicate the values as recorded in the dataset table, whereas the corresponding names without this underscore indicate the same values as referred to in the text. For example, k_plant_sapwood corresponds to $k_{plant_sapwood}$, and k_plant_leaf corresponds to k_{plant_leaf}.

(50.93%), followed by stem heat balance (24.05%), compensation heat pulse (13.40%), heat ratio (4.51%) and transient thermal dissipation (4.21%) (Fig. 3).

The proportions of observations with available data for each plant trait were: height (61.08%), DBH (52.25%), plant basal area (54.80%), leaf area (33.30%), sapwood area (25.28%), Huber value (23.35%), and age (57.07%). For stand-level characteristics, data availabilities were: LAI (33.35%), stand density (36.87%), and stand basal area (20.54%). Value ranges for all the variables are provided in Table 5.

Technical Validation

Multiple sources of error could affect the quality of the k_{plant} data compiled in the dataset. One source of uncertainty is the data extraction itself, as some data were digitised from published figures using WebPlotDigitizer. WebPlotDigitizer minimises digitisation error, by performing careful axis calibration and zooming in to increase cursor precision. Digitisation precision was tested using 10 synthetic plots (5 bar charts, 5 scatter plots) with known true Y-axis values spanning the typical range of k_{plant_leaf} (1×10^{-6} to 1×10^{-4} kg m^{-2} s^{-1} MPa^{-1}) (https://github.com/vflo/Kplant_database/blob/main/digitalization_error_evaluation.R). Each synthetic plot was digitised by 4 independent observers. A linear mixed model was fitted to the digitisation error (digitised minus true value) with observer and plot as crossed random intercepts. The mean digitisation bias was -6.5×10^{-9} kg m^{-2} s^{-1} MPa^{-1} (95% CI: -5.4×10^{-8} to 4.1×10^{-8}), not significantly different from zero, indicating no systematic over- or underestimation. The total standard deviation of digitisation error, combining between-observer ($\sigma = 3.8 \times 10^{-8}$ kg m^{-2} s^{-1} MPa^{-1}), between-plot ($\sigma = 4.2 \times 10^{-8}$ kg m^{-2} s^{-1} MPa^{-1}) and residual ($\sigma = 1.1 \times 10^{-7}$ kg m^{-2} s^{-1} MPa^{-1}) variability, was 1.2×10^{-7} kg m^{-2} s^{-1} MPa^{-1} (0.12% of the Y-axis range).

For studies that did not report whole-plant hydraulic conductance directly, k_{plant} was calculated using Eq. 1. In some cases, a small temporal mismatch between *F* and $\Delta\Psi$ measurements may also introduce additional uncertainty. In addition, uncertainties in *F* and/or $\Delta\Psi$ could propagate into the final estimates of k_{plant}. These uncertainty estimates are provided only in the original units reported by each study and were not converted across normalisation levels. When standard errors (SE) for k_{plant} were not reported in the original sources, these were calculated as follows:

Field name	Definition	Data type	Units	Possible range	Number of unique records
IDref	Reference identifier	numeric	—	—	357
si_country	Country name	factor	—	(-90,90)	40
si_lat	Latitude in decimal format	numeric	decimal degrees	(-180,180)	290
si_long	Longitude in decimal format	numeric	decimal degrees	—	298
si_altitude	Altitude above sea level	numeric	m	—	164
si_site	Code characterising each site/sub-site (or population) within a study	string	—	—	327
si_treatment	Treatment of the measures	string	—	(-90,90)	458
Date	Date of the measure	factor	YYYYMMDD	—	1024

Table 4. Site, treatment and measurement time metadata.

Field name	Definition	Data type	Units	Possible range	Number of observations	Median	Range
pl_name	Name/code of the plant	string	—	—	397	—	—
pl_species_original*	Species scientific name as in the source	string	—	—	495	—	—
pl_family	Family name	string	—	—	100	—	—
gbif_id	GBIF unique numeric identifier	string	—	—	424	—	—
pl_species_corrected	Corrected species name	string	—	—	425	—	—
pl_genus	Genus of the species	string	—	—	245	—	—
pl_growth_form*	Plant growth form	factor	—	—	7	—	—
pl_age_mean	Average age of the samples	numeric	year	>0	2192	8	0–708
pl_height_mean	Average plant height for the target species	numeric	M	>0	2346	7.8	0.1–82
pl_basal_area_mean	Average basal area	numeric	m^2	>0	2105	0.0224	0–16.62
pl_DBH_mean	Average diameter at breast height in trees or average stem diameter in other plant forms	numeric	Cm	>0	2007	17.3	0.2–460
pl_LA_mean	Average plant leaf area	numeric	m^2	>0	1279	6.94	1×10^{-4}–4102
pl_SA_mean	Average sapwood area	numeric	m^2	>0	971	0.012	5.73×10^{-6}–1.23
pl_huber_value_mean	pl_SA/pl_LA	numeric	$m^2\ m^{-2}$	>0	897	6.00×10^{-4}	7.98×10^{-6}–0.066
SA_methods	Method used to estimate Sapwood area	factor	—	—	1157	—	—
pl_devstage*	Developmental stage	factor	—	—	3760	—	—
pl_experimental_conditions*	Experimental conditions	factor	—	—	3841	—	—
st_basal_area	Stand basal area	numeric	$m^2\ ha^{-1}$	—	789	27.3	0.77–339.74
st_LAI	Leaf area index	numeric	$m^2\ m^2$	>0	1281	2.66	0.10–16.54
st_density	Stand tree density	numeric	plants ha^{-1}	—	1416	1425	20–1×10^6
LAI_methods	Method used to estimate LAI	factor	—	—	1070	—	—

Table 5. Plant-scale and Stand-scale characteristics. Compulsory variables are marked with an asterisk (*).

$$SE_K = |K| \sqrt{\left(\frac{SE_F}{F}\right)^2 + \left(\frac{SE_\Delta\psi}{\Delta\psi}\right)^2} \quad (7)$$

F measurements originate from leaf-, stem-, and whole-plant scales, each associated with specific methodological uncertainties. At the leaf scale, gas-exchange systems based on Infrared gas analysers may be affected by non-steady state conditions, imperfect chamber sealing, and uncertainties in boundary-layer conductance and leaf temperature[35]. For instance, measurements of air and leaf temperature using LI-6400XT can show systematic bias affecting estimates of stomatal conductance[36]. Porometers infer stomatal conductance from water vapour diffusion within a small and rapidly perturbed microclimate chamber, making them sensitive to humidity fluctuations, equilibration time, and leakage[37]. At the stem scale, sap flow methods carry uncertainties associated with probe installation, wounding effects, sensor parameterisation, radial and circumferential sap-velocity variability affecting the upscaling of point measurements to whole-stem flow[29,38]. A further source of uncertainty is that sap flow may lag behind or deviate from actual canopy-level transpiration because internal water capacitance buffers short-term fluxes, potentially leading to an underestimation of k_{plant}[39]. At the whole-plant scale, gravimetric methods provide accurate estimates of *F*, but container-based measurements may restrict root growth and alter soil-plant boundary conditions, potentially biasing flux estimates relative to field conditions[40]. These uncertainties are largely unavoidable at the dataset level, and method-level biases cannot be corrected retrospectively. They are expected to contribute to between-study variation in k_{plant} and should therefore be considered when comparing results across studies.

Field name	Definition	Data type	Unit	Possible range	Number of records
soil_sand_perc	Soil sand percentage	numeric	%	—	1391
soil_silt_perc	Soil silt percentage	numeric	%	—	1320
soil_clay_perc	Soil clay percentage	numeric	%	—	1417
soil_om_perc	Soil organic matter percentage	numeric	%	—	377
soil_bulk_density	Bulk density of the soil	numeric	cg cm^{-3}	—	549
soil_type	Soil category based on the dominant size of the particles within a soil.	string	—	—	2329
g_s	stomatal conductance per unit leaf area during measurement	numeric	mol m^{-2} s^{-1}	>0	944
E	transpiration per unit leaf area during measurement	numeric	mmol m^{-2} s^{-1}	>0	515
VPD	Vapour pressure deficit recorded during measurement	numeric	kPa	>0	692
CO_2	Atmospheric CO_2 concentration	numeric	ppm	>0	186
P_{50}	Availability of water potential at 50% loss of hydraulic conductivity data	factor	—	—	261
P_{min}	Availability of Minimum water potential data	factor	—	—	402
TLP	Availability of Turgor loss point data	factor	—	—	231
G_{smax}	Availability of maximum stomatal conductance data	factor	—	—	562
K_s	Availability of shoot hydraulic conductivity data	factor	—	—	460

Table 6. Soil information, concurrent environmental and physiological measurements, and data availability of other hydraulic traits in the original publications.

Field name	Definition
Contributor	Name of contributor who extracted the data from the paper
Reference_title	Title of the paper
Source	DOI or reference of the paper
Observations	Any further observation regarding methodological issues

Table 7. Dataset details.

Source level \ Target level	k_{plant}	k_{plant_leaf}	$k_{plant_sapwood}$	k_{plant_wood}	k_{plant_ground}
k_{plant}	—	pl_LA	pl_SA	pl_basal_area	st_density
k_{plant_leaf}	pl_LA	—	pl_huber_value	—	pl_LAI
$k_{plant_sapwood}$	pl_SA	pl_huber_value	—	—	—
k_{plant_wood}	pl_basal_area	—	—	—	—
k_{plant_ground}	st_density	pl_LAI	—	—	—

Table 8. Whole-plant hydraulic conductance normalisation level conversions and mediators.

Estimation of k_{plant} also requires measurements of Ψ_{leaf}. In most studies, Ψ_{leaf} was measured on excised tissues using a pressure chamber, which provides functionally relevant estimates that are compatible with transpiration and sap-flow measurements[41,42]. A smaller subset of observations relied on dew-point psychrometers, applied either to excised tissues or *in situ*. While psychrometers can be highly precise under controlled conditions, they are sensitive to temperature gradients and tissue-level biases, particularly under field conditions, and therefore require experienced operators to obtain reliable data[43]. Gravitational effects are also an important component of $\Delta\Psi$, but no additional correction was applied to k_{plant} calculations in this dataset. Gravitational effects based on canopy height are typically already been accounted for in studies calculating $\Delta\Psi$ from Ψ_{soil} and Ψ_{midday}, and cancel out when $\Delta\Psi$ is calculated from $\Psi_{predawn}$ and Ψ_{midday} measured at similar heights.

Potential errors also arise depending on whether k_{plant} was calculated using ratio-based or slope-based approaches. Ratio-based estimates represent instantaneous apparent k_{plant} and are sensitive to non-steady-state effects and errors in Ψ_{leaf} when gradients are very small. Internal water storage causes stem sap flow to lag behind canopy transpiration, resulting in time-dependent bias in k_{plant} estimates. In contrast, slope-based estimates integrate multiple observations across a range of Ψ_{leaf} (generally within a single day) and typically provide a more robust characterisation of whole-plant hydraulic efficiency for that period, although hysteretic behaviour may still influence these estimates because they are less sensitive to individual measurements. However, because they integrate measurements over several hours, they may be less directly comparable to instantaneous mid-day estimates, and hysteretic behaviour may still influence the resulting estimates. Despite these differences, discrepancies between the two approaches are expected to be small under comparable conditions[44]. To assess agreement between methods, we compared ratio-based (k_{plant_ratio}) and slope-based (k_{plant_slope}) estimates across 9

Dataset metadata	Description
KPLANT_dataset.csv	Main dataset containing all k_{plant} observations and metadata
Extraction_template.xlsx	Standardised template used for data extraction
Extraction_protocol. docx	Standardised protocol used for data extraction
Individual_studies.zip	Compressed Zip file containing individual.xlsx studies
Qc_reports.zip	Compressed Zip file containing HTML reports for individual datasets

Table 9. Database repository structure.

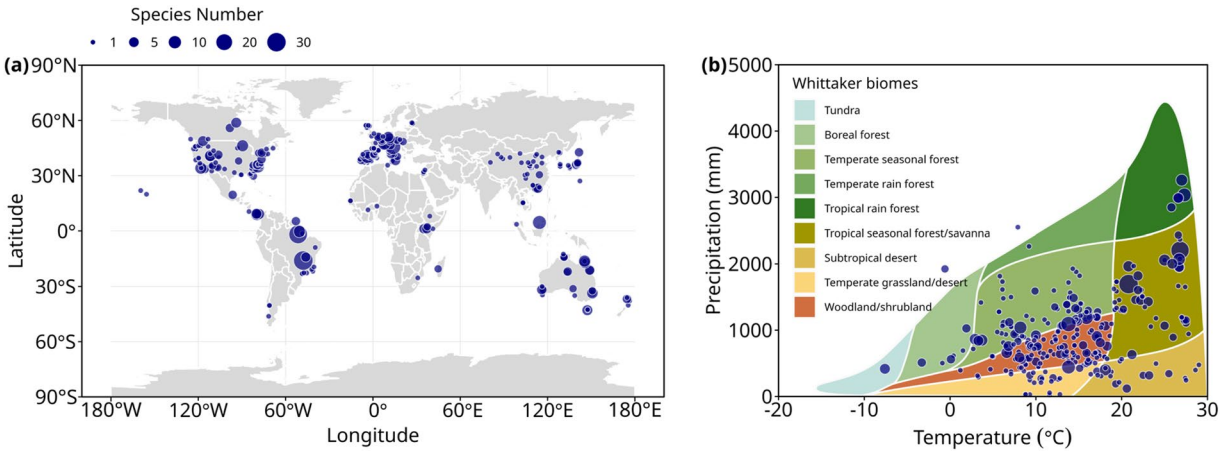


Fig. 2 (**a**) Geographic distribution and (**b**) Whittaker biomes distribution of the k_{plant} measures under field conditions included in the dataset. The size of the dots in (**a**) and (**b**) show the number of species available at each location.

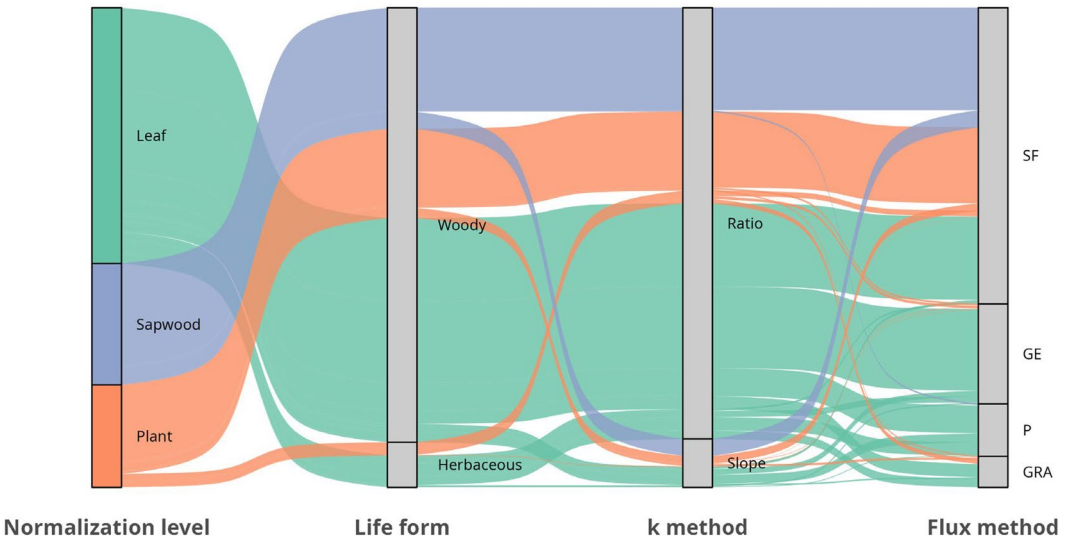


Fig. 3 Sankey diagram illustrating the distribution of plant records in the dataset across normalisation levels (Leaf, Sapwood, and Plant), major life forms (Woody, Herbaceous), k_{plant} calculation methods (Ratio and Slope), and water-flow measurement method, comprising GE (gas exchange), P (porometer), GRA (gravimetry), and sap flow methods (SF). Each colour represents a different original normalisation level. Categories with relatively few records were omitted for clarity, including high-pressure flow meter (HPFM) in the Flux method (17 records), and wood (23 records) and ground (24 records) in the normalisation level.

data sources reporting both. The ratio of k_{plant_ratio} to k_{plant_slope} ranged from 0.76 to 1.44 (Table 10), indicating that method-related discrepancies can reach up to 44%.

Additional uncertainty could arise from the conversion of k_{plant} across normalisation levels (k_{plant_leaf}, $k_{plant_sapwood}$, k_{plant_wood}, k_{plant_ground}, k_{plant}), which relied on the accuracy and precision of the scaling ratios, the normality of

IDref	normalisation_level	k_{plant_ratio}	k_{plant_slope}	k_{plant_ratio} / k_{plant_slope}
70	Sapwood	1.02×10^{-5}	7.70×10^{-6}	1.33
471	Sapwood	3.39×10^{-6}	2.35×10^{-6}	1.44
557	Plant	1.47×10^{-6}	1.52×10^{-6}	0.97
803	Leaf	6.27×10^{-4}	5.30×10^{-4}	1.18
804	Leaf	1.38×10^{-4}	1.55×10^{-4}	0.89
1212	Sapwood	6.42×10^{-2}	5.00×10^{-2}	1.28
1235	Leaf	5.57×10^{-5}	7.34×10^{-5}	0.76
1248	Plant	9.93×10^{-4}	9.55×10^{-4}	1.04
1661	Leaf	2.99×10^{-5}	3.79×10^{-5}	0.79

Table 10. Comparison of ratio- and slope-based estimates of k_{plant} for matched observations.

plant size trait distributions, and the allometric relationships used to convert among traits. Uncertainties associated with these traits reflect methodological differences in their measurement and variation in their temporal dynamics. For example, optical gap-fraction methods tend to underestimate leaf area index (LAI) due to leaf clumping and saturation at high canopy densities[45,46], while LAI estimates derived from litter-trap depend on phenology, sampling design, and species identity[47]. Allometric relationships embed site- and species-specific assumptions that may not remain stable over time and not hold across environmental gradients[48,49]. Sapwood area measurements may include non-conductive tissue when All_sapwood is used rather than Only_conductive_part, leading to underestimation of sapwood-specific hydraulic conductance and over-estimation of Huber Values[50].

Plant-level size traits were sometimes derived from stand-level data combined with plant density. In some cases, reported forest density refers to the entire stand rather than the target species. This can introduce additional uncertainty during scaling, particularly in more diverse stands where the potential error is likely to be greater. These uncertainties primarily affect absolute k_{plant} values, while relative patterns, such as responses along environmental gradients and scaling relationships with plant size, are expected to be more robust.

Data availability

The dataset generated is available in the Zenodo repository at https://doi.org/10.5281/zenodo.19816125. The repository includes the main data file containing all k_{plant} observations and metadata (KPLANT_database.csv), a standardised data extraction template (Extraction_template.xlsx), the extraction protocol (Extraction_protocol.docx), a compressed zip file containing all the quality controlled individual studies in.xlsx format (Individual_studies.zip), and a compressed zip file with dataset-specific quality control reports (Qc_reports.zip) (Table 9). Full details of file contents and variable definitions are provided in the Data Records section and associated tables. All files are provided under a Creative Commons Attribution 4.0 International (CC BY 4.0) licence.

Code availability

The R code used to generate the quality control reports described in this study is publicly available on GitHub at https://github.com/vflo/Kwp_QC. The repository contains scripts implementing the automated quality control procedure, including the three checks described in the Methods section, and produces the dataset-specific HTML reports provided in the Qc_reports.zip file. All the code used to merge the final dataset and to create the figures is publicly available on GitHub at https://github.com/vflo/Kplant_database.

Received: 4 May 2026; Accepted: 29 September 2026;
Published: xx xx xxxx

References

1. Shi, H. Potential of constructing all-encompassing soil–plant-atmosphere-continuum stations and datasets from meteorological, flux, soil moisture station networks and plant-relevant observations. *Hydrological Processes* **38**, e15284 https://doi.org/10.1002/hyp.15284 (2024).
2. Torres-Ruiz, J. M. *et al*. Plant hydraulics at the heart of plant, crops and ecosystem functions in the face of climate change. *New Phytologist* **241**, 984–999 https://doi.org/10.1111/nph.19463 (2024).
3. Tyree, M. T. & Ewers, F. W. The hydraulic architecture of trees and other woody plants. *New Phytologist* **119**, 345–360 https://doi.org/10.1111/j.1469-8137.1991.tb00035.x (1991).
4. Mencuccini, M., Manzoni, S. & Christoffersen, B. Modelling water fluxes in plants: from tissues to biosphere. *New Phytologist* **222**, 1207–1222 https://doi.org/10.1111/nph.15681 (2019).
5. McCulloh, K. A., Domec, J. C., Johnson, D. M., Smith, D. D. & Meinzer, F. C. A dynamic yet vulnerable pipeline: Integration and coordination of hydraulic traits across whole plants. *Plant, Cell & Environment* **42**, 2789–2807 https://doi.org/10.1111/pce.13607 (2019).
6. Adams, H. D. *et al*. A multi-species synthesis of physiological mechanisms in drought-induced tree mortality. *Nature Ecology & Evolution* **1**, 1285–1291 https://doi.org/10.1038/s41559-017-0248-x (2017).
7. Anderegg, W. R. *et al*. Tree mortality from drought, insects, and their interactions in a changing climate. *New Phytologist* **208**, 674–683 https://doi.org/10.1111/nph.13477 (2015).
8. Sperry, J. S. & Tyree, M. T. Mechanism of water stress-induced xylem embolism. *Plant Physiology* **88**, 581–587 https://doi.org/10.1104/pp.88.3.581 (1988).
9. Meinzer, F. C. Co-ordination of vapour and liquid phase water transport properties in plants. *Plant, Cell & Environment* **25**, 265–274 https://doi.org/10.1046/j.1365-3040.2002.00781.x (2002).

10. Mencuccini, M. The ecological significance of long-distance water transport: short-term regulation, long-term acclimation and the hydraulic costs of stature across plant life forms. *Plant, Cell & Environment* **26**, 163–182 https://doi.org/10.1046/j.1365-3040.2003.00991.x (2003).
11. Sabot, M. E. B. *et al*. Plant profit maximization improves predictions of European forest responses to drought. *New Phytologist* **226**, 1638–1655 https://doi.org/10.1111/nph.16376 (2020).
12. Hawkins, L. R. *et al*. Comparing Model Representations of Physiological Limits on Transpiration at a Semi-Arid Ponderosa Pine Site. *Journal of Advances in Modeling Earth Systems* 14. https://doi.org/10.1029/2021ms002927 (2022).
13. Sperry, J. S. *et al*. Predicting stomatal responses to the environment from the optimization of photosynthetic gain and hydraulic cost. *Plant, Cell & Environment* **40**, 816–830 https://doi.org/10.1111/pce.12852 (2017).
14. Venturas, M. D., Sperry, J. S. & Hacke, U. G. Plant xylem hydraulics: What we understand, current research, and future challenges. *Journal of Integrative Plant Biology* **59**, 356–389 https://doi.org/10.1111/jipb.12534 (2017).
15. Domec, J.-C., Lachenbruch, B., Pruyn, M. L. & Spicer, R. Effects of age-related increases in sapwood area, leaf area, and xylem conductivity on height-related hydraulic costs in two contrasting coniferous species. *Annals of Forest Science* **69**, 17–27 https://doi.org/10.1007/s13595-011-0154-3 (2012).
16. Liu, Y., Holtzman, N. M. & Konings, A. G. Global ecosystem-scale plant hydraulic traits retrieved using model–data fusion. *Hydrology and Earth System Sciences* **25**, 2399–2417 https://doi.org/10.5194/hess-25-2399-2021 (2021).
17. Zhang, Z., Guan, H., Veneklaas, E., Singha, K. & Batelaan, O. Revealing seasonal plasticity of whole-plant hydraulic properties using sap-flow and stem water-potential monitoring. *Hydrology and Earth System Sciences* **29**, 3975–3992 https://doi.org/10.5194/hess-29-3975-2025 (2025).
18. Domec, J. C. *et al*. Decoupling the influence of leaf and root hydraulic conductances on stomatal conductance and its sensitivity to vapour pressure deficit as soil dries in a drained loblolly pine plantation. *Plant, Cell & Environment* **32**, 980–991 https://doi.org/10.1111/j.1365-3040.2009.01981.x (2009).
19. Sack, L. & Holbrook, N. M. Leaf hydraulics. *The Annual Review of Plant Biology* **57**, 361–381 https://doi.org/10.1146/annurev.arplant.56.032604.144141 (2006).
20. Steudle, E. Water uptake by roots: effects of water deficit. *Journal of Experimental Botany* **51**, 1531–1542 https://doi.org/10.1093/jexbot/51.350.1531 (2000).
21. Win, K. T., Oo, A. Z., Ookawa, T., Kanekatsu, M. & Hirasawa, T. Changes in hydraulic conductance cause the difference in growth response to short-term salt stress between salt-tolerant and -sensitive black gram (Vigna mungo) varieties. *Journal of Plant Physiology* **193**, 71–78 https://doi.org/10.1016/j.jplph.2016.02.013 (2016).
22. West, G. B., Brown, J. H. & Enquist, B. J. A general model for the structure and allometry of plant vascular systems. *Nature* **400**, 664–667 https://doi.org/10.1038/23251 (1999).
23. Couvreur, V. *et al*. Water transport through tall trees: A vertically explicit, analytical model of xylem hydraulic conductance in stems. *Plant, Cell & Environment* **41**, 1821–1839 https://doi.org/10.1111/pce.13322 (2018).
24. Olson, M. E. *et al*. Universal hydraulics of the flowering plants: vessel diameter scales with stem length across angiosperm lineages, habits and climates. *Ecology Letters* **17**, 988–997 https://doi.org/10.1111/ele.12302 (2014).
25. Maseda, P. H. & Fernandez, R. J. Stay wet or else: three ways in which plants can adjust hydraulically to their environment. *Journal of Experimental Botany* **57**, 3963–3977 https://doi.org/10.1093/jxb/erl127 (2006).
26. Wolfe, B. T. *et al*. Leaves as bottlenecks: The contribution of tree leaves to hydraulic resistance within the soil-plant-atmosphere continuum. *Plant, Cell & Environment* **46**, 736–746 https://doi.org/10.1111/pce.14524 (2023).
27. Wankmüller, F. J. P. *et al*. Global influence of soil texture on ecosystem water limitation. *Nature* **635**, 631–638 https://doi.org/10.1038/s41586-024-08089-2 (2024).
28. Peters, R. L. *et al*. Uniform regulation of stomatal closure across temperate tree species to sustain nocturnal turgor and growth. *Nature Plants* **11**, 725–730 https://doi.org/10.1038/s41477-025-01957-3 (2025).
29. Poyatos, R. *et al*. Global transpiration data from sap flow measurements: the SAPFLUXNET database. *Earth System Science Data* **13**, 2607–2649 https://doi.org/10.5194/essd-13-2607-2021 (2021).
30. Liu, Y. Scaling plant hydraulic traits to predict ecosystem fluxes under drought. *New Phytologist* **250**, 2078–2084 https://doi.org/10.1111/nph.71114 (2026).
31. De Kauwe, M. G. *et al*. Towards species-level forecasts of drought-induced tree mortality risk. *New Phytologist* **235**, 94–110 https://doi.org/10.1111/nph.18129 (2022).
32. Chamberlain, S. A. & Szocs, E. taxize: taxonomic search and retrieval in R. *F1000Res* **2**, 191 https://doi.org/10.12688/f1000research.2-191.v2 (2013).
33. GBIF Secretariat. GBIF Backbone Taxonomy. *Checklist dataset accessed via GBIF.org on 2026-05-02*. https://doi.org/10.15468/39omei (2023).
34. Zhao, Y. *et al*. Global dataset of plant water transport capacity. *Zenodo* https://doi.org/10.5281/zenodo.19816125 (2026).
35. Busch, F. A. *et al*. A guide to photosynthetic gas exchange measurements: Fundamental principles, best practice and potential pitfalls. *Plant, Cell & Environment* **47**, 3344–3364 https://doi.org/10.1111/pce.14815 (2024).
36. Garen, J. C. *et al*. Gas exchange analysers exhibit large measurement error driven by internal thermal gradients. *New Phytologist* **236**, 369–384 https://doi.org/10.1111/nph.18347 (2022).
37. Toro, G., Flexas, J. & Escalona, J. M. Contrasting leaf porometer and infra-red gas analyser methodologies: an old paradigm about the stomatal conductance measurement. *Theoretical and Experimental Plant Physiology* **31**, 483–492 https://doi.org/10.1007/s40626-019-00161-x (2019).
38. Flo, V., Martinez-Vilalta, J., Steppe, K., Schuldt, B. & Poyatos, R. A synthesis of bias and uncertainty in sap flow methods. *Agricultural and Forest Meteorology* **271**, 362–374 https://doi.org/10.1016/j.agrformet.2019.03.012 (2019).
39. Meinzer, F. C., James, S. A. & Goldstein, G. Dynamics of transpiration, sap flow and use of stored water in tropical forest canopy trees. *Tree Physiology* **24**, 901–909 https://doi.org/10.1093/treephys/24.8.901 (2004).
40. Beeson, R. C. Weighing lysimeter systems for quantifying water use and studies of controlled water stress for crops grown in low bulk density substrates. *Agricultural Water Management* **98**, 967–976 https://doi.org/10.1016/j.agwat.2011.01.005 (2011).
41. Rodriguez-Dominguez, C. M. *et al*. Leaf water potential measurements using the pressure chamber: Synthetic testing of assumptions towards best practices for precision and accuracy. *Plant, Cell & Environment* **45**, 2037–2061 https://doi.org/10.1111/pce.14330 (2022).
42. Turner, N. C. Measurement of plant water status by the pressure chamber technique. *Irrigation Science* **9**, 289–308 https://doi.org/10.1007/bf00296704 (1988).
43. Jones, H. G. Monitoring plant and soil water status: established and novel methods revisited and their relevance to studies of drought tolerance. *Journal of Experimental Botany* **58**, 119–130 https://doi.org/10.1093/jxb/erl118 (2007).
44. Cochard, H., Bréda, N. & Granier, A. Whole tree hydraulic conductance and water loss regulation in Quercus during drought: evidence for stomatal control of embolism? *Annales des Sciences Forestières* **53**, 197–206 https://doi.org/10.1051/forest:19960203 (1996).
45. Chen, J. M., Rich, P. M., Gower, S. T., Norman, J. M. & Plummer, S. Leaf area index of boreal forests: Theory, techniques, and measurements. *Journal of Geophysical Research: Atmospheres* **102**, 29429–29443 https://doi.org/10.1029/97jd01107 (1997).
46. Weiss, M., Baret, F., Smith, G. J., Jonckheere, I. & Coppin, P. Review of methods for *in situ* leaf area index (LAI) determination. *Agricultural and Forest Meteorology* **121**, 37–53 https://doi.org/10.1016/j.agrformet.2003.08.001 (2004).

47. Jonckheere, I. *et al*. Review of methods for *in situ* leaf area index determination. *Agricultural and Forest Meteorology* **121**, 19–35 https://doi.org/10.1016/j.agrformet.2003.08.027 (2004).
48. Arias, D., Calvo-Alvarado, J. & Dohrenbusch, A. Calibration of LAI-2000 to estimate leaf area index (LAI) and assessment of its relationship with stand productivity in six native and introduced tree species in Costa Rica. *Forest Ecology and Management* **247**, 185–193 https://doi.org/10.1016/j.foreco.2007.04.039 (2007).
49. Jonckheere, I., Muys, B. & Coppin, P. Allometry and evaluation of *in situ* optical LAI determination in Scots pine: a case study in Belgium. *Tree Physiology* **25**, 723–732 https://doi.org/10.1093/treephys/25.6.723 (2005).
50. Clearwater, M. J., Meinzer, F. C., Andrade, J. L., Goldstein, G. & Holbrook, N. M. Potential errors in measurement of nonuniform sap flow using heat dissipation probes. *Tree Physiology* **19**, 681–687 https://doi.org/10.1093/treephys/19.10.681 (1999).

Author contributions

Y.Z., V.F., M.M., and J.M.V. designed the dataset. Y.Z. and V.F. coordinated the work, performed quality control, and drafted the manuscript. Y.Z., S.A., A.A.-R., M.D.C., E.C., D.Ch, M.D.G., S.H., E.M., M.Mo, L.R., M.Si, P.S., L.W.S., A.Te, A.To, A.T.T., F.V.B., and V.F. classified the collection of sources. Y.Z., B.A.M., L.Ad, L.D.L.A., W.R.L.A., C.B., P.B., O.B., A.C., D.Ch, H.C., M.D.G., L.F.U., A.F.S., A.G., T.G., C.G., V.H.S., S.H., Y.H., K.M.J., Y.L., M.Ma, I.M., N.M.S.P., J.M.V., L.R.M., C.M.C., R.Pe, R.Po, J.A.R.-V., M.Sa, P.S.M., C.S., L.Sc, S.T., A.V., L.V., C.Z., J.W., and V.F. extracted the data. L.R.M., R.Pe, R.Po, J.A.R.-V., Y.S., I.A., D.Cr, T.D., J.D., J.M.V., N.D., F.C.D., J.C.D., C.E., D.I.F., P.F., A.K., J.M.L., P.M., K.N., P.L.P., C.P., Y.P., R.L.S., and F.Va provided publicly available data sources. All coauthors reviewed the final version of the manuscript.

Funding

Funding was provided by the Spanish Ministry of Science and Universities, MICIU/AEI/10.13039/501100011033, with the 'Severo Ochoa' Centres of Excellence programme, Ref. CEX2023-001340-S (awarded to VF); project DRASTIC, PID2022-137270NB-I00 (awarded to MM); and projects CNS2023-143618 (awarded to JAR-V) and RYC2021-031759-I (awarded to TG), both co-funded by the "European Union NextGenerationEU/PRTR". This publication was also supported by the China Scholarship Council (202406270163) (awarded to YZ). ND, JML and NMSP received funding from French ANR (TAW-tree, ANR-23-CE01-0008). CS received funding by an Investissement d'Avenir grant from the Agence Nationale de la Recherche (CEBA: ANR-10-LABX-25-01). CZ received financial support from the French government in the framework of the IdEX Bordeaux University "Investments for the Future" program/GPR Bordeaux Plant Sciences. ATT acknowledges funding from the Gordon and Betty Moore Foundation 13283 and the National Science Foundation 2003205. DCh received the support of a fellowship from the "la Caixa" Foundation (ID 100010434; code LCF/BQ/PI25/12100008). KMJ was funded by the European Union on a Marie Skłodowska-Curie Actions (MSCA) Postdoctoral fellowship, 101107177—IVERdrought. Views and opinions expressed are, however, those of the author(s) only and do not necessarily reflect those of the European Union or the MSCA. Neither the European Union nor the granting authority can be held responsible for them. LDLA acknowledges funding from the US National Science Foundation 2003205, 2516844, 2316522. JMV benefited from an ICREA Academia Award. YS and LR were supported by UK Natural Environment Research Council grant NE/V000071/1. TD, JD and CP acknowledge funding by FCT – Fundação para a Ciência e a Tecnologia, I.P., through the projects UID/00239/2025 (DOI: 10.54499/UID/00239/2025) and UID/PRR/00239/2025 (DOI: 10.54499/UID/PRR/00239/2025) of the Forest Research Centre.

Competing interests

The authors declare no competing interests.

Additional information

Correspondence and requests for materials should be addressed to Y.Z. or V.F.

Reprints and permissions information is available at www.nature.com/reprints.

Publisher's note Springer Nature remains neutral with regard to jurisdictional claims in published maps and institutional affiliations.

Open Access This article is licensed under a Creative Commons Attribution-NonCommercial-NoDerivatives 4.0 International License, which permits any non-commercial use, sharing, distribution and reproduction in any medium or format, as long as you give appropriate credit to the original author(s) and the source, provide a link to the Creative Commons licence, and indicate if you modified the licensed material. You do not have permission under this licence to share adapted material derived from this article or parts of it. The images or other third party material in this article are included in the article's Creative Commons licence, unless indicated otherwise in a credit line to the material. If material is not included in the article's Creative Commons licence and your intended use is not permitted by statutory regulation or exceeds the permitted use, you will need to obtain permission directly from the copyright holder. To view a copy of this licence, visit http://creativecommons.org/licenses/by-nc-nd/4.0/.

© The Author(s) 2026

This Article in Press is shared early to give you faster access to new research. It is citable and carries a permanent DOI. The final edited version will replace it automatically.

Yanchao Zhao[1,2]✉, Maurizio Mencuccini[2,3], Belén Acuña-Míguez[4], Lucette Adet[2], Shadman Amin[5], Alba Anadon-Rosell[6,7], Leander D. L. Anderegg[8], William R. L. Anderegg[9], Ismael Aranda[10], Christoph Bachofen[11], Paulo Bittencourt[12], Oliver Binks[2], Miquel De Cáceres[13], Andrea Carminati[14], Eva Castells[2,15], David Chaparro[2], Hervé Cochard[16], Danielle Creek[17], Teresa David[18], Jorge David[18], Nicolas Delpierre[19], Margaux Didion-Gency[2], Frederic C. Do[20], Jean-Christophe Domec[21,22], Cleiton Eller[23], Laura Fernández-de-Uña[24], David I. Forrester[25], Patrick Fonti[11], Alicia Forner-Sales[26,27], Alice Gauthey[28,29], Teresa E. Gimeno[2], Charlotte Grossiord[30,31], Virginia Hernandez-Santana[32], Sonia Hernando[2], Ying Hu[33], Kate M. Johnson[2], Ansgar Kahmen[34], Yating Li[35], Jean-Marc Limousin[36], Marylou Mantova[37], Isabelle Maréchaux[38], Evan Margiotta[5], Nicolas Martin-StPaul[4], Jordi Martinez-Vilalta[2,15], Lion R. Martius[39], Christopher McCarthy[40], Patrick Meir[41], Maé Moriggia[42], Kim Novick[43], Pablo Luis Peri[44], Richard L. Peters[45], Clara A. Pinto[18,46], Rafael Poyatos[2,15], Yakir Preisler[47], Jose Alberto Ramirez-Valiente[10], Lucy Rowland[48], Manon Sabot[33], Yann Salmon[49,50], Roberto L. Salomón[51], Pablo Sanchez-Martinez[39], Leonie Schönbeck[52], Mateus Silva[48], Pol Soler[2], Clément Stahl[53], Laura W. Stewart[2], Abiel Teixidó[2,15], Ambra Tosto[48], Santiago Trueba[38], Anna T. Trugman[5], Aude Valade[20], Fernando Valladares[27], Fernanda De Vasconcellos Barros[48], Léa Veuillen[4,36], Jingwei Wu[1], Camille Ziegler[54] & Victor Flo[2,15]✉

[1]State Key Laboratory of Water Resources Engineering and Management, Wuhan University, Wuhan, 430072, Hubei, China. [2]Ecological and Forestry Applications Research Center CREAF, Campus UAB, 08193, Bellaterra, Catalonia, Spain. [3]ICREA, Passeig Lluís Companys 23, 08010, Barcelona, Spain. [4]INRAE-URFM, Domaine Saint Paul - 228 route de l'Aerodrome - Site Agroparc - CS 40509, Avignon, Cedex 9, 84914, France. [5]University of California Santa Barbara, Department of Geography, Santa Barbara, CA, 93106, USA. [6]Departament de Biologia Evolutiva, Ecologia i Ciències Ambientals, Universitat de Barcelona, Barcelona, Spain. [7]Institut de Recerca de la Biodiversitat (IRBio), Universitat de Barcelona, Barcelona, Spain. [8]Department of Ecology, Evolution & Marine Biology, University of California Santa Barbara, Santa Barbara, CA, 93117, USA. [9]School of Biological Sciences, University of Utah, Salt Lake City, UT, 84103, USA. [10]ICIFOR-INIA-CSIC, Ctra. La Coruña Km 7.5, 28040, Madrid, Spain. [11]Forest and Soil Ecology, Swiss Federal Institute for Forest, Snow and Landscape Research WSL, CH-1015, Lausanne, Switzerland. [12]School of Earth and Environmental Sciences, Cardiff University, Cardiff, CF10 3AT, UK. [13]CSIC - CREAF, Cerdanyola del Vallès, Catalonia, 08290, Spain. [14]Institute of Terrestrial Ecosystems, ETH Zurich, Zurich, Switzerland. [15]Universitat Autònoma de Barcelona, E08193, Bellaterra (Cerdanyola del Vallès), Catalonia, Spain. [16]Université Clermont Auvergne, INRAE, PIAF, 63000, Clermont-Ferrand, France. [17]Faculty of Environmental Sciences and Natural Resource Management, Norwegian University of Life Sciences, P.O. Box 5003, Ås, 1432, Norway. [18]CEF-ISA, University of Lisbon PT, Lisbon, Portugal. [19]Université Paris-Saclay, CNRS, AgroParisTech, Ecologie Société Evolution, Gif-sur-Yvette, 91190, France. [20]Eco&Sols, Univ Montpellier, CIRAD, INRAE, Institut Agro, IRD, Montpellier, France. [21]Bordeaux Sciences AGRO, UMR1391 ISPA INRA, 1 Cours du General de Gaulle, Gradignan, 33175, Cedex, France. [22]Nicholas School of the Environment, Duke University, Durham, 27708, NC, USA. [23]Department of Plant Biology, Institute of Biology, CP 6109, University of Campinas - UNICAMP, Campinas, SP, 13083-970, Brazil. [24]Universidade de Vigo, Department of Plant Biology and Soil Sciences, 32004, Ourense, Spain. [25]CSIRO Environment, GPO Box 1700, ACT, 2601, Canberra, Australia. [26]International University of La Rioja (UNIR) ES, Logroño, Spain. [27]Laboratorio Internacional de Cambio Global (LINCGlobal), Departamento Biogeografía y Cambio Global, Museo Nacional de Ciencias Naturales, MNCN-CSIC, E-28006, Madrid, Spain. [28]Birmingham Institute of Forest Research, University of Birmingham, Edgbaston, B15 2TT, UK. [29]School of Geography, Earth and Environmental Sciences, University of Birmingham, Edgbaston, B15 2TT, UK. [30]Plant Ecology Research Laboratory PERL, School of Architecture, Civil and Environmental Engineering, EPFL, 1015, Lausanne, Switzerland. [31]Functional Plant Ecology, Forest and Soil Ecology Unit, Swiss Federal Institute for Forest, Snow and Landscape WSL, Lausanne, Switzerland. [32]Plant Ecophysiology and Irrigation Group, Instituto de Recursos Naturales y Agrobiología (IRNAS), Consejo Superior de Investigaciones Científicas (CSIC), Seville, Spain. [33]Max Planck Institute for Biogeochemistry, 07745, Jena, Germany. [34]Department of Environmental Sciences-Botany, University of Basel, Basel, Switzerland. [35]State Key Laboratory of Tibetan Plateau Earth System, Environment and Resources (TPESER), Institute of Tibetan Plateau Research, Chinese Academy of Sciences, Beijing, China. [36]CEFE, Univ Montpellier, CNRS, EPHE, IRD, Montpellier, France. [37]Université Clermont-Auvergne, INRAE, PIAF, Clermont-Ferrand, France. [38]AMAP, Univ Montpellier, IRD, CIRAD, CNRS, INRAE, Montpellier, 34398, France. [39]School of GeoSciences, University of Edinburgh, King's Buildings, Alexander Crum Brown Rd, Edinburgh, EH9 3FF, UK. [40]School of Natural Sciences, University of Tasmania, Private Bag 55, Tas, Hobart, 7001, Australia. [41]School of Geosciences, University of Edinburgh, Edinburgh, UK. [42]Department of Environmental Systems Science, ETH Zurich, Zurich, Switzerland. [43]O'Neill School of Public and Environmental Affairs, Indiana University - Bloomington, Indiana, USA. [44]Instituto Nacional de Tecnología Agropecuaria (INTA), Universidad Nacional de la Patagonia Austral (UNPA)-CONICET, Río Gallegos, Santa Cruz, Argentina. [45]Tree Growth and Wood Physiology, TUM School of Life Sciences, Technical University of Munich, Hans-Carl-v.-Carlowitz-Platz 2, 85354, Freising, Germany. [46]National Institute for Agricultural and Veterinary Research (INIAV, I.P.) PT, Oeiras, Portugal. [47]Plant Science Institute, The Agriculture Research Organization - Volcani Center, Hamaccabim 68, Rishon Lezion, Israel. [48]Department of Geography, Faculty of Environment Science and Economy, University of Exeter, Exeter, UK. [49]Institute for Atmospheric and Earth System

Research (INAR), Faculty of Sciences, University of Helsinki, Gustaf Hällströmin katu 2, PO Box 64, FI-00014, Helsinki, Finland. [50]Department of Forest Sciences, Institute for Atmospheric and Earth System Research (INAR), Faculty of Agriculture and Forestry, University of Helsinki, Latokartanonkaari 7, PO Box 27, FI-00014, Helsinki, Finland. [51]Departamento de Sistemas y Recursos Naturales, Research Group FORESCENT, Universidad Politécnica de Madrid, Madrid, Spain. [52]Southern Swedish Forest Research Centre, Swedish University of Agricultural Sciences, Alnarp, Sweden. [53]INRAE, UMR Ecofog, AgroParisTech, Cirad, CNRS, Universite des Antilles, Universite de Guyane, 97387, Kourou, France. [54]University of Bordeaux, INRAE, UMR BIOGECO, Pessac, 33615, France. ✉e-mail: zhaoyanchao@whu.edu.cn; v.flo@creaf.uab.cat